Activated Carbon Material Made From Apricot Stones as Highly Pseudocapacitive Electrode Material for Hybrid Supercapacitor

B.P. Bakhmatyuk[1], I.Ya. Dupliak[1], I.M. Budzulyak[2], B.I. Rachiy[2]

[1] *Lviv Polytechnic National University, 12 Bandera Street, Lviv 79013, Ukraine*
[2] *Vasyl Stefanyk Prycarpathian National University, 57 Shevchenka Street, Ivano-Frankivsk 76018, Ukraine*

Bimodal activated carbon material made from apricot stones (ACMAS) have been investigated as polarized electrode for a hybrid supercapacitor (HS). Analysis of frequency dependence of impedance at the ACMAS│ZnI$_2$ interface under its anode polarization of 0.35 V–0.46 V has been made. The plotted dependence of specific pseudocapacitance (C$_P$) on electrode potential (E) takes its maximal value 13600 F g^{-1} at E = 0.46 V. Galvanostatic discharge (GD) at the current density (i) 1.0 A g^{-1} ensures the value 13235 F g^{-1}. Dependences of Faradaic resistance (R$_F$) and time constant (τ) on anode polarization of ACMAS electrode have been determined.

Keywords: Hybrid supercapacitor; Pseudocapacitance; Nyguist diagram.

1. INTRODUTION

Carbon materials are used in wide range of applications depending on their chemical inertness, structural strength, high electric conductivity, polarizability. Among them, porous carbon materials are very popular as electrode materials for electrochemical supercapacitors (ES), Li secondary battery, fuel cell, dye sensitized solar cell [1]. In the work [2], it is shown that the process of iodine electrosorption by microporous ACM in the system of HS can be well described by Langmuir model with small contribution of interatomic interaction (g) in the adsorption layer. For ACM, the calculated maximal theoretical values of specific charge (q$_I$) and C$_P$ for $g = 0$ takes the values of 0.76 C·m^{-12} and 7.4 F·g^{-1} respectively. The aim of this work is the investigation of pseudocapacitive characteristics of ACMAS of bimodal porous structure in the system of HS.

2. METHODOLOGY

2.1 Obtaining of activated carbon material

The ACMAS obtaining was carried out in two stages. The first stage: the initial raw materials were under heat treatment without air to remove evaporated components of the material and to form primary porosity; material carbonization was conducted in a medium of water vapor under the pressure of $(12 - 15) \cdot 10^5$ Pa at 1153 K for $3 - 4$ hour. The second stage: to increase the specific surface area and to purify the material from admixtures, the obtained carbon was activated in boiling layer. The material was put into a reactor for activation with subsequent holding for 2.7 hours in a gas stream (a mixture of hot air and argon) in the temperature range of $573 - 873$ K. Specific surface areas and pore size dispertion of the carbon sample were determined by means of N$_2$ adsorption at 77 K using a Quantachrome apparatus.

2.2 Electrochemical measurements and electrode preparation

Zn foil (99.999%, Aldrich) and ZnI$_2$ ($\geq$ 98%, Aldrich) were used for our experiments. All the chemicals were of analytical grade; therefore, they were used without further purification. Galvanostatic and impedance (in the frequency range of 10^{-13} to 3×10^4 Hz with the amplitude 5 mV at controlled potential conditions) dependencies have been determined with a help of AUTOLAB measuring complex made in Netherlands by "ECO CHEMIE" in combination with FRA-2 and GPES computer programs. Impedance data, obtained at the measuring, have been simulated in accordance with electric equivalent circuits (EEC) using ZView 2.3 (Scribner Associates) package. The capacitance values necessary for plotting the farad–volt dependence have been determined from an imaginary part of the impedance locus at a frequency of 10^{-3} Hz according to the formula: $C = -(j2\pi f\, Z'')^{-1}$ with the accuracy of 2–8% (Kramers-Kroning's test estimated was within 10^{-6} to 10^{-5}). For our investigations, there were used film-like electrodes with active mass $m_a = 1 - 2$ mg ($S = 0.5$ cm^2) with the added binder 5-10 wt.% of Teflon and 10-20 wt.% of acetylene carbon black or graphite for increase in electric conductance. The electrodes had been assembled by pressing them to a net of stainless steel. Electrochemical investigations were carried out in two-electrode system and three-electrode glass cells with a Zn counter electrode (16 cm^2) and with a AgCl│Cl$^-$ reference electrode. As the electrolyte, 25 % ZnI$_2$ aqueous solution was used. All measurements were taken at room temperature. The electrodes potentials (E) are referred to the standard hydrogen electrode.

3. RESULTS AND DISCUSSION

3.1 Porometry

Figure 1 a,b shows nitrogen adsorption/desorption isotherms (Fig. 1a) and PSD curves of ACMAS (Fig.1b). The type IV is ascribed to these isotherms of ACMAS, they have an obvious hysteresis loop for P/P_0 from 0.42 to 0.9, and this indicates the existence of a large percentage of mesopores [3].

When the P/P_0 is below 0.1, the presence of the distinguishable amount of adsorbed nitrogen indicates that the samples have some micropores. The sizes of
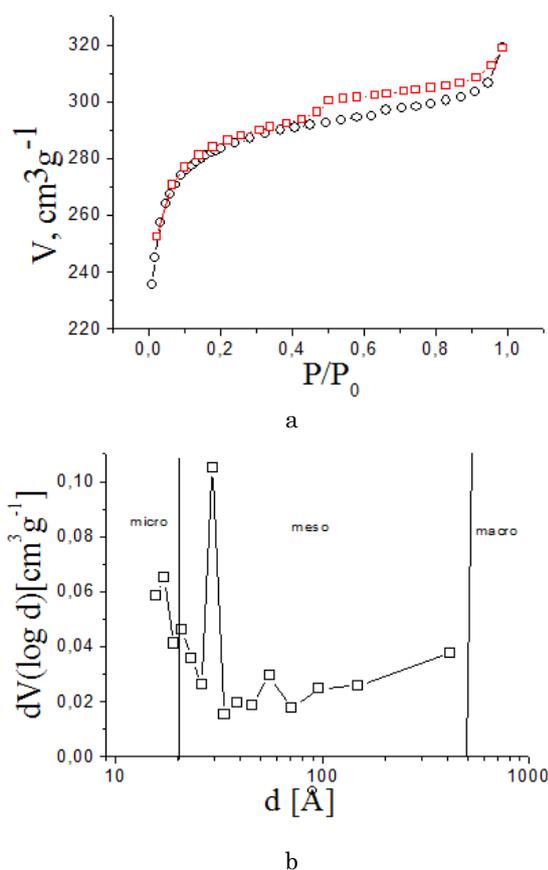
a

b

Fig. 1 – N$_2$ adsorption – desorption isotherms (a), pore size distributions (b) of ACMAS

the pores of the sample are mainly concentrated within the diameter range of 1.5-5 nm, and the ion radius of iodine (0.23 nm [2]) is much less.

The ACMAS possess a relatively centralized PSD and bimodal distribution of 1.56 to 2 nm micropores in combination with large fraction of 2 to 5 nm mesopores. The total specific surface area ($TSA = S_{micro} + S_{meso}$) of ACMAS was 1076 m^{2}g^{-1} and the total pore volume 0.493 cm^3 g^{-1}. The average pores size of this sample was 2.94 nm. As far as capacitor's electrode material is concerned, mesoporous carbons combined with certain amount of micropores are beneficial to improving both energy density and power density.

3.2 Electrochemical properties

To evaluate the characteristics of the synthesized ACMAS as an electrode material for supercapacitors, it was tested in asymmetric two-electrode system using aqueous ZnI$_2$ electrolyte, which is the prototype of a hybrid supercapacitor (HS) in charged state [2]:

$$Zn | 25\% \ ZnCl_2 | C_x^*I \qquad (3.1)$$
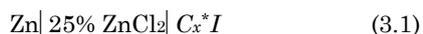
This corresponds to the current generating process:

$$C_x^*I + 0.5 \ Zn = C_x^* + I + 0.5 \ Zn^{2+} \qquad (3.2)$$
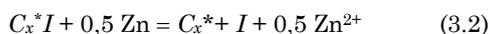
The process which proceeds during anode polarization of ACMAS in 25% ZnI$_2$ to an electrode potential of 0.46 V, which is less than the potential of iodine release into free state 0.536 V and that of

formation of the redox couple $I^-_3/3I^-$, is considered in this work as processes of electrosorption of I^- (transition of I^- into adatomic state under an underpotential relative to the main reaction) according to the scheme from [2]:

$$C_x^*I + e^- \overset{K}{=} C_x^* + I^-, \qquad (3.3)$$
$$\theta \qquad E \quad 1-\theta \quad c_{I^-}$$
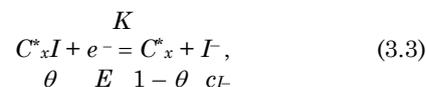
where C_x^* is the surface of the carbon material, x is the number of carbon atoms per one iodine atom, θ is fractional coverage by I at C_x^*; K is the constant of adsorption equilibrium; c_{I^-} is the concentration of iodine ions in the solution

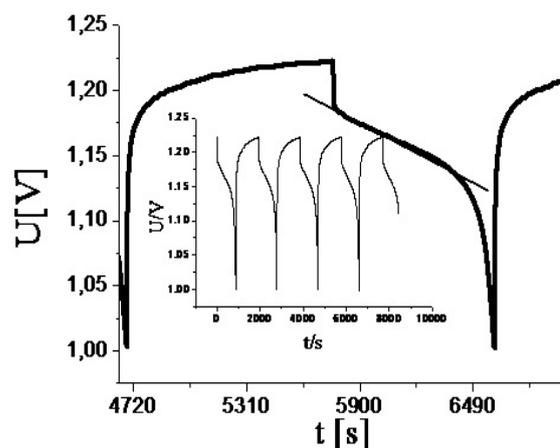**Fig. 2** – Typical galvanostatic charge – discharge (GCD) profiles of the prepared activated carbons at 1.0 A·g^{-1} current density

Fig. 2 shows the typical galvanostatic charge - discharge (GCD) profiles of the prepared activated carbons at 1.0 A·g^{-1} current density. The measured value of charge voltage U_c ($U_c = 1.222$ V) (Fig. 2) of the prototype of a HS (1) is less than 1.3 V, which is for Zn|I$_2$ galvanic couple. Galvanostatic discharge (GD) at a polarization ΔU ($\Delta U = 1.19$ V - 1.0 V = 0.19 V) shows the value of electrosorption specific capacity 827 C g^{-1}. The GD at $\Delta U = 1.184$ V - 1.133 V = 0.051 V corresponds to linear the segment of galvanostatic cycle, it shows the value of the discharge C_P ($C_P = 675$ C g^{-1}× (0.051 V)$^{-1}$ = 13235 F g^{-1} (12.4 F m^{-2})). The obtained value of discharge specific capacity (C) 675 C·g amounts to 83% of its maximal theoretical value $C = 0.76$ C·m^{-2}·1074 m^2·g^{-1} = 816 C·g^{-1} for the investigated material ACMAS.

The typical Nyquist diagrams (impedance spectrum) of $C_x^*I | 25\%ZnI_2$ interface are shown in Fig.3 a,b. The imaginary part of the impedance (-Z'') as a function of the ohmic resistance (Z') consists of two characteristic parts. They consist of semicircles (for high frequencies 79 Hz-4.5 × 10^4 Hz) and straight lines with a slope of 60° - 86° (for low frequencies 10^{-3} Hz -79 Hz). It can be seen that the diameters of the semicircles dercreased at $E = 0.46$ V, indicating that the electrode can effectively reduce the charge transfer resistance to 1.4 Ohm ×cm^2. In the range of 0.35V to 0.46 V, the R_F values determined in such way are reduced from 1.8 Ohm × cm^2 to 1.4 Ohm × cm^2, R_s insignificantly changes.
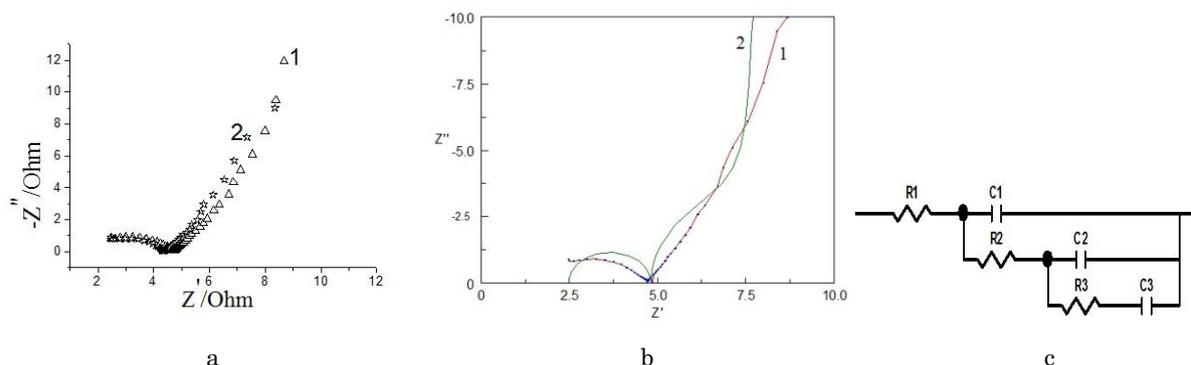
Fig. 3 – Nyquist diagrams The Nyquist plots (a) of ACMAS electrode at $E = 0.43$ V(1), $E = 0.46$ V (2). Nyquist plots (b) of ACMAS electrode at $E = 0.46$ V according to experimental (curve 1) and according to EEC (curve 2) and. EEC of the ACMAS⎪25% ZnI$_2$ interface (c)

According to [4], the straight lines with a slope of 60° - 86° in low frequency region 10^{-3} Hz - 79 Hz of Nyquist plot are caused by pseudocapacitance (C_p), which is generated at the electrode surface. It can be seen in (Fig.4a) that the $(\omega Z'')^{-1}$ value is not constant but strongly depends on the frequency. Fig. 4 a lists the $(\omega Z'')^{-1}$ values calculated from the impedance spectra, taken for charged electrode. In all cases, at the lowest frequency 1 mHz the $(\omega Z'')^{-1}$ value is close to the nominal electrode capacitance. At higher frequencies, the $(\omega Z'')^{-1}$ value significantly decreases. The positive polarization of the electrode from $C = 0.35$ V to $E = 0.46$ V leads to almost 40 – times greater increase in capacitance, from $C = 344$ F g^{-1} to C$_P$ = 13600 F g^{-1} (12.7 F m^{-2}) at the least frequency $f = 10^{-3}$ Hz. This is possible due to pseudocapacitive mechanism of the electrode charging. According to the measured data of capacitance at the frequency of 10^{-3} Hz, the dependence of specific pseudocapacitance on electrode potential ($C_P - E$) is plotted (Fig 4b). This C_P –E dependence takes its maximal value of 12.7 F m^{-2} (13600 F g^{-1}) at $E = 0.46$ V. The increase in the value of C_P to 12.4 F m^{-2}-12.7 F m^{-2} is caused by the influence of interatomic interaction (g) in the adsorption layer (g ≈-3) according to the known formula [4]:

$$C_F = q_I F \cdot (RT)^{-1} \theta (1 - \theta) \cdot (1 + g\,\theta(1 - \theta))^{-1} \quad (3.4)$$

Small deviation of the experimental data from the modeled ones is obtained for transmission line circuit with pore size distribution (TLC-PSD) (Fig.3b) [5].

According to TLC-PSD (Fig.3c), the chain R_1-C_1 represents the resistance and capacitance of pores of the range 4 - 5 nm. The chains R_2-C_2 and R_3-C_3 represent resistances and capacitances of ACMAS micro- and mesopores of two ranges as to their diameters $3 - 4$ nm and 1.5 nm - 3 nm. At $E = 0.46$ V, pseudocapacitive contribution of ACMAS meso- and micropores increases in following sequence: $C_2 = 4846$ F·g^{-1}, $C_3 = 8954$ F·g^{-1}, and the total specific pseudocapacitance C_T ($C_T = 13800$ F·g^{-1}). The time constants of of ACMAS meso- and micropores at $E = 0.46$ V take the values of 14 s, and 43 s.

4. CONCLUSION

The bimodal ACMAS is made from apricot stones. Good capacitive and kinetic parameters of the process of iodine electrosorption at C_x^*I⎪25% ZnI$_2$ interface under the anode polarization of 0.35 to 0.46 V have been studied in this work. Super high values of C$_P$ where obtained from the data of impedance and galvanostatic measurements. Comparison of practical and theoretical values of C and C$_P$ confirm the mechanism of proceeding of the investigating process according to Frumkin model of adsorption. All of the results indicate that highly porous activated carbon can be easily synthesized from apricot stones or other biological waste for commercial use as electrode materials for hybrid supercapacitor.

REFERENCES

1. E. Frackowiak, F. Beguin, *Supercapacitors: Materials, System and Applications* (Wiley-VCH: 2013).
2. B.P. Bakhmatyuk, *Electrochim. Acta* 163, 167 (2015).
3. X. He, P. Ling, J. Qiu, M. Zheng, *J. Power Source* **240**, 109 (2013).
4. B.E. Conway, *Electrochemical Supercapacitors* (NewYork: Kluwer-Plenum Pub. Co: 1999).
5. H.K. Song, H.Y. Hwang, K.H. Lee, L.H. Dao, *Electrochim. Acta* **45**, 2241 (2000).